

Pt₂ dimer anchored vertically in defective BN monolayer as an efficient catalyst for N₂ reduction: A DFT study

Linke Yu and Fengyu Li *

Physical School of Science and Technology, Inner Mongolia University, Hohhot 010021, China

* Correspondence: fengyuli@imu.edu.cn

Table S1. The distance between metal atoms (D , in Å), the binding energies (E_b) of metal atoms in 10 species, the cohesive energy (E_{coh}) of bulk M (in eV), and the $E_b - E_{coh}$ (in eV).

system	D	E_b	E_{coh}	$E_b - E_{coh}$
Co ₂ ⊥ vb-BN	2.40	−5.49	−5.04	−0.45
Ni ₂ ⊥ vb-BN	2.37	−5.62	−5.04	−0.58
Rh ₂ ⊥ vb-BN	2.78	−5.60	−5.93	0.33
Ir ₂ ⊥ vb-BN	2.85	−5.80	−7.59	1.79
Pt ₂ ⊥ vb-BN	2.92	−4.53	−5.52	0.99
Co ₂ ⊥ vn-BN	2.30	−4.30	−5.04	0.74
Ni ₂ ⊥ vn-BN	2.48	−5.11	−5.04	−0.07
Rh ₂ ⊥ vn-BN	2.76	−5.63	−5.93	0.30
Ir ₂ ⊥ vn-BN	3.24	−6.04	−7.59	1.55
Pt ₂ ⊥ vn-BN	2.99	−6.31	−5.52	−0.79

Table S2. The Bader charge (Q , in $|e|$) on the M atoms, the magnetic order (MO) and the magnetic moment on M atoms (M , in μ_B) of the stable catalyst structures.

system	Q (M/M')	MO	M (M ₁ /M ₂)
Co ₂ ⊥vb-BN	+0.84/+0.84	AFM	1.97/−1.14
Ni ₂ ⊥vb-BN	+0.76/+0.76	FM	0.40/0.40
Rh ₂ ⊥vb-BN	+0.50/+0.50	FM	0.36/0.36
Pt ₂ ⊥vb-BN	+0.44/+0.44	FM	0.26/0.26
Co ₂ ⊥vn-BN	+0.15/+0.15	FM	0.61/0.61
Ni ₂ ⊥vn-BN	−0.05/−0.05	NM	0.00/0.00
Rh ₂ ⊥vn-BN	−0.25/−0.25	FM	0.45/0.45
Pt ₂ ⊥vn-BN	−0.48/−0.48	FM	0.14/0.14

Table S3. The adsorption energy (E_{ad} , in eV), the charge transferred from the stable DACs to the adsorbed N₂ (ΔQ , in $|e|$), the shortest distance between the N₂ and M (d , in Å), the distance between the N atom and N atom in N₂ (d_{N-N} , in Å) of the N₂ molecule adsorbed on the stable catalyst structures.

system	E_{ad}	ΔQ	d	d_{N-N}
Co ₂ ⊥vb-BN	−1.26	−0.43	1.92/2.00	1.17
Rh ₂ ⊥vb-BN	−0.89	−0.35	2.07/2.23	1.16
Pt ₂ ⊥vb-BN	−1.11	−0.35	2.11/2.11	1.17
Rh ₂ ⊥vn-BN	−1.26	−0.30	2.13/2.22	1.15

Table S4. The $E_{zpe} - TS$ of the free gas molecules.

$E_{zpe} - TS$ (eV)	
NH ₃	0.42
H ₂ O (l)	0.00
H ₂	-0.05
N ₂	-0.35

Table S5. Free energy correction ($E_{zpe} - TS$) (in eV) for each adsorbed species in the NRR reaction path on Co₂ \perp vb-BN, Rh₂ \perp vb-BN, Pt₂ \perp vb-BN and Rh₂ \perp vn-BN.

	*N ₂	*NNH	*NHNH	*NHNH ₂	*NH ₂ NH ₂	*NH ₂ ...NH ₃	*NH ₃
Co ₂ \perp vb-BN	0.09	0.36	0.69	1.04	1.33	1.42	0.96
	*N ₂	*NNH	*NHNH	*NHNH ₂	*NH ₂ NH ₂	*NH ₂ ...NH ₃	*NH ₃
Rh ₂ \perp vb-BN	0.09	0.35	0.72	1.07	1.34	1.47	0.94
	*N ₂	*NNH	*NHNH	*NHNH ₂	*NH ₂ NH ₂	*NH ₂ ...NH ₃	*NH ₃
Pt ₂ \perp vb-BN	0.09	0.41	0.72	1.10	1.42	1.48	0.97
	*N ₂	*NNH	*NHNH	*NHNH ₂	*NH ₂ NH ₂	*NH ₂ ...NH ₃	*NH ₃
Rh ₂ \perp vn-BN	0.09	0.40	0.69	1.09	1.37	1.42	0.96

Table S6. The potential-determining steps, and limiting potentials (U_L) for the NRR on the stable catalyst structures.

System	Potential-determining step	U_L (in V)
Co ₂ ▯vb-BN	*NHNH ₂ → *NH ₂ NH ₂	−0.69
Rh ₂ ▯vb-BN	*NN → *NNH	−0.50
Pt ₂ ▯vb-BN	*NN → *NNH	−0.06
Rh ₂ ▯vn-BN	*NN → *NNH	−0.49
Rh@vb-BN	*NN → *NNH	−1.25
Pt@vb-BN	*NN → *NNH	−0.35
Rh@vn-BN	*NN → *NNH	−1.48

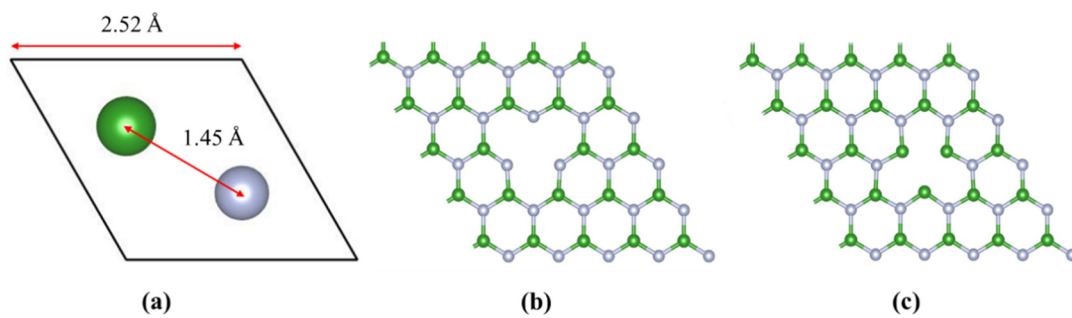


Figure S1. Structural diagram of the single-cell structure of (a) *h*-BN, (b) vb-BN and (c) vn-BN model. Colour scheme: B, green and N, silver.

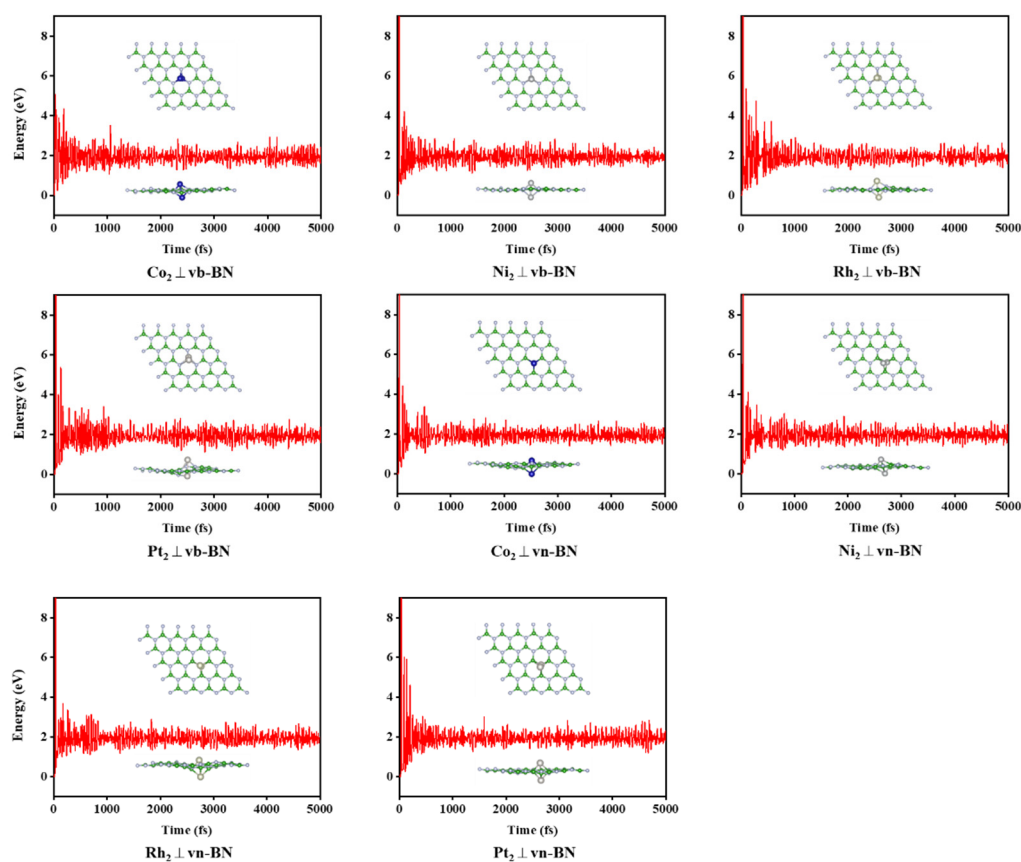


Figure S2. The energy evolution of 8 catalysts during 5 ps FPMD simulations at 300 K, the insets are the final annealed structures.

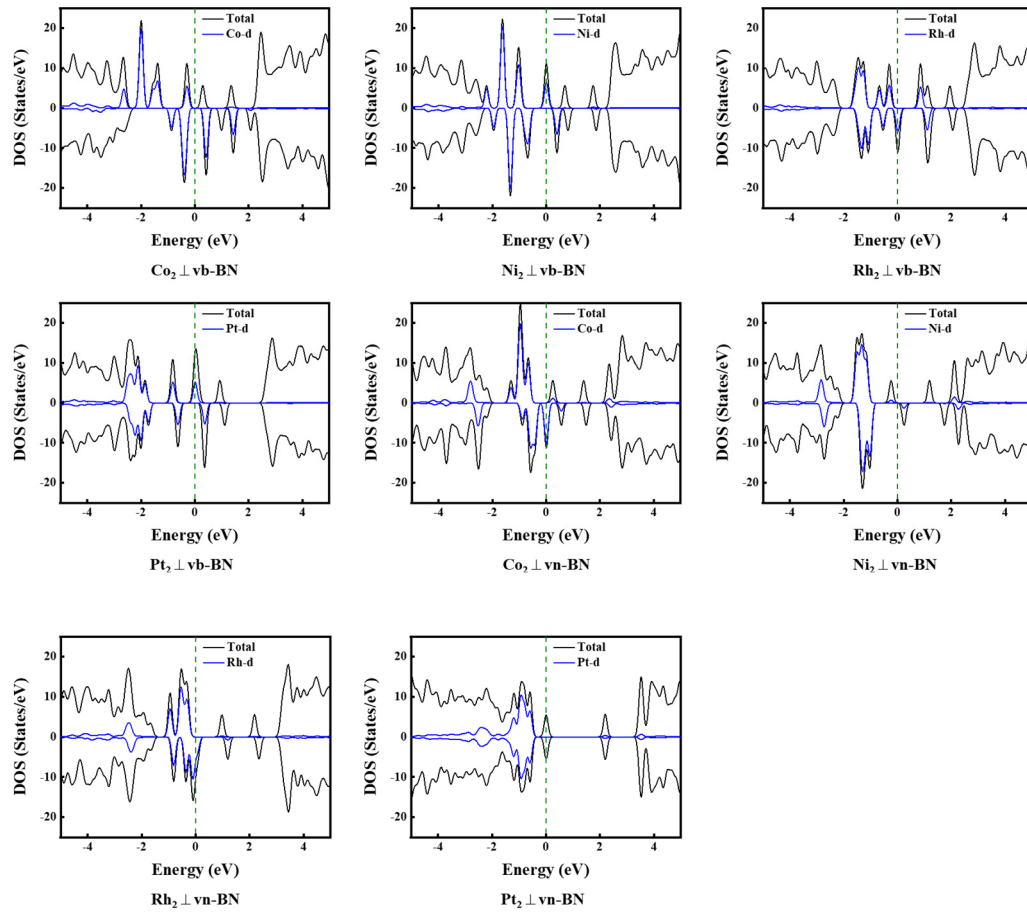


Figure S3. Density of states (DOS) of 8 DACs. The green dashed lines indicate the Fermi energy level.

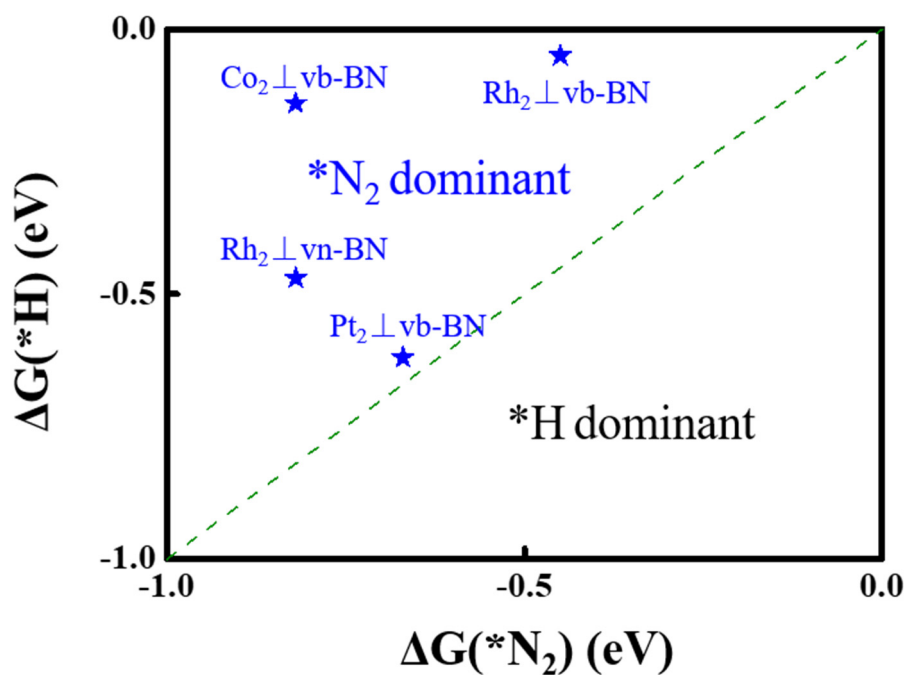


Figure S4. Calculated $\Delta G(*N_2)$ and $\Delta G(*H)$ on 4 DACs.

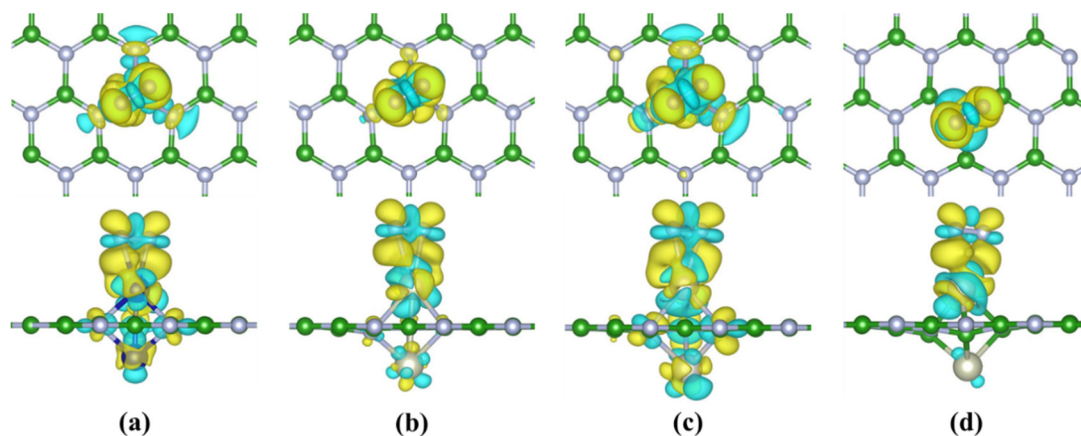


Figure S5. Differential charge diagram of N_2 -adsorbed on (a) $Co_2 \perp vb-BN$, (b) $Rh_2 \perp vb-BN$, (c) $Pt_2 \perp vb-BN$ and (d) $Rh_2 \perp vn-BN$. Yellow is positively charged, blue is negatively charged. The isosurface value was set as $0.003 \text{ e}/\text{\AA}^{-3}$.

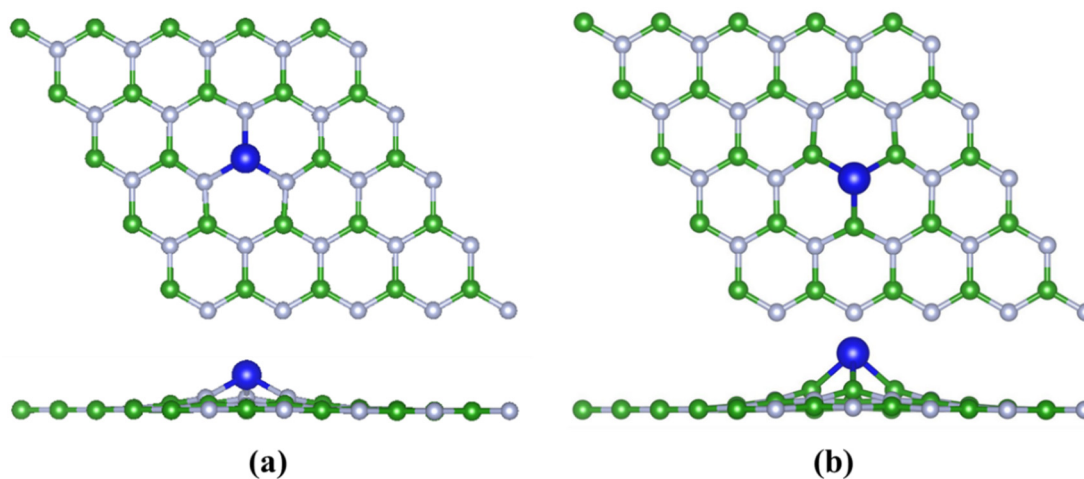


Figure S6. Structural diagram of the (a) M@vb-BN and (b) M@vn-BN model. Colour scheme: B, green; N, silver; M, blue.

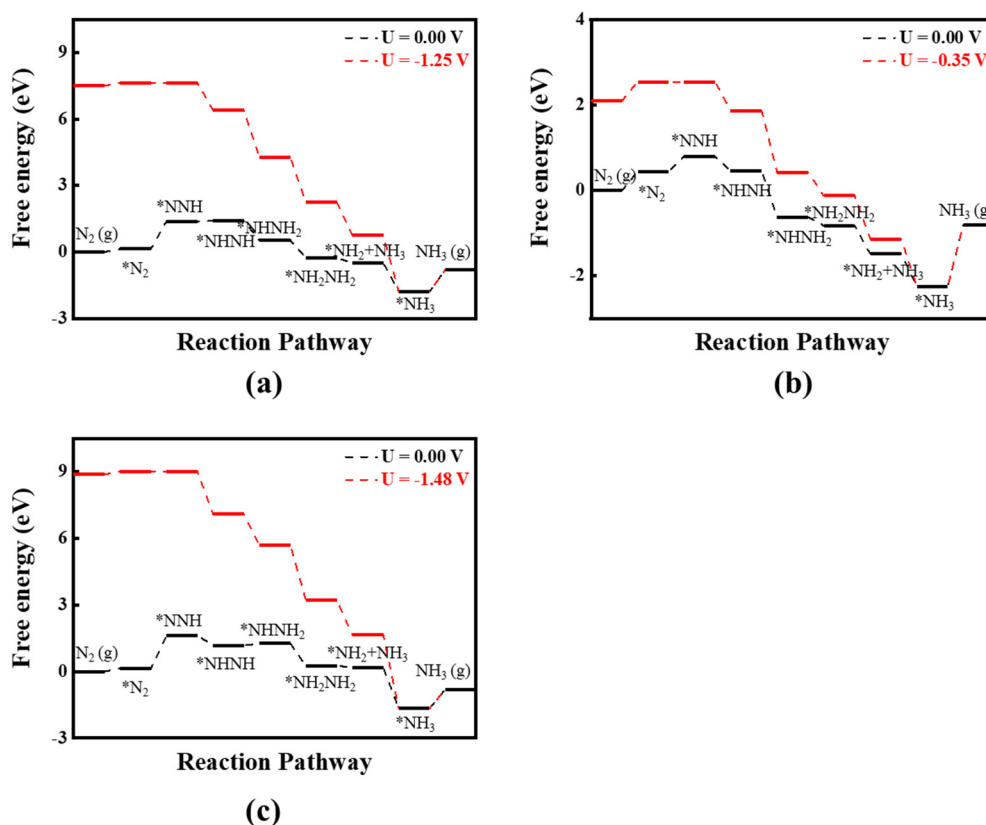


Figure S7. Free energy diagram of NRR on (a) Rh@vb-BN, (b) Pt@vb-BN and (c) Rh@vn-BN catalyst at zero and applied potential (limiting potential) through the enzymatic mechanism.

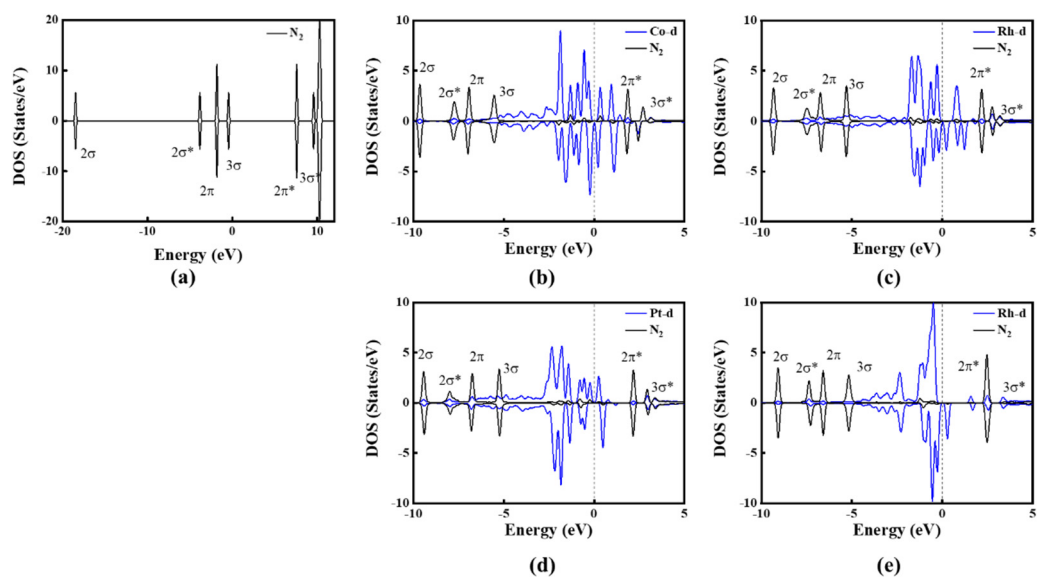


Figure S8. (a) Molecular orbitals of free N₂. The projected density of states (PDOS) of (b) Co₂ \perp vb-BN, (c) Rh₂ \perp vb-BN, (d) Pt₂ \perp vb-BN and (e) Rh₂ \perp vn-BN.

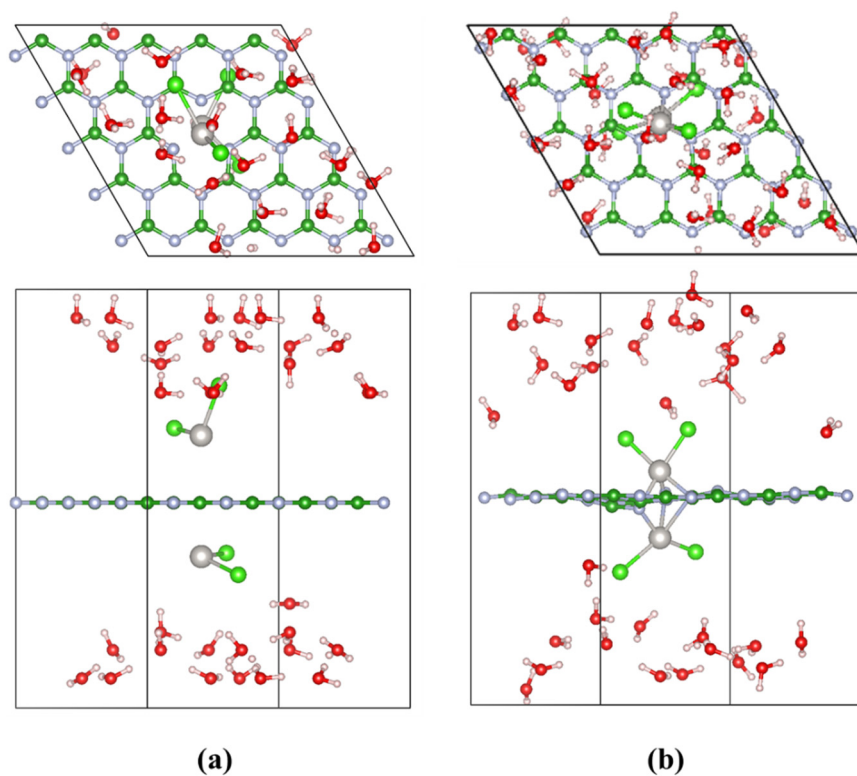


Figure S9. Top and side views of the snapshots of atomic configurations of FAMD simulations for the synthetic process of Pt₂ \perp vb-BN (a,b). The model consists of a 5 \times 5 \times 1 supercell of BN with a boron vacancy, two PtCl₂ molecules and 34 water molecules. Pt, N, B, H, O and Cl are indicated by gray, silver, dark green, white, red and light green, respectively.